THE JOURNAL OF BIOLOGICAL CHEMISTRY VOL. 284, NO. 52, pp. 36700–36710, December 25, 2009

β Integrin Tyrosine Phosphorylation Is a Conserved Mechanism for Regulating Talin-induced Integrin Activation*[S]

Received for publication, September 5, 2009, and in revised form, October 9, 2009 Published, JBC Papers in Press, October 20, 2009, DOI 10.1074/jbc.M109.061275

Nicholas J. Anthis[‡1], Jacob R. Haling[§], Camilla L. Oxley[‡], Massimiliano Memo[‡], Kate L. Wegener[‡], Chinten J. Lim[§], Mark H. Ginsberg[§], and Iain D. Campbell[‡2]

From the [‡]Department of Biochemistry, University of Oxford, South Parks Road, Oxford OX1 3DR, United Kingdom and the [§]Department of Medicine, University of California, San Diego, La Jolla, California 92093

Integrins are large membrane-spanning receptors fundamental to cell adhesion and migration. Integrin adhesiveness for the extracellular matrix is activated by the cytoskeletal protein talin via direct binding of its phosphotyrosine-binding-like F3 domain to the cytoplasmic tail of the β integrin subunit. The phosphotyrosine-binding domain of the signaling protein Dok1, on the other hand, has an inactivating effect on integrins, a phenomenon that is modulated by integrin tyrosine phosphorylation. Using full-length tyrosine-phosphorylated ^{15}N-labeled β3, β1A, and β7 integrin tails and an NMR-based protein-protein interaction assay, we show that talin1 binds to the NP*X*Y motif and the membrane-proximal portion of β3, β1A, and β7 tails, and that the affinity of this interaction is decreased by integrin tyrosine phosphorylation. Dok1 only interacts weakly with unphosphorylated tails, but its affinity is greatly increased by integrin tyrosine phosphorylation. The Dok1 interaction remains restricted to the integrin NP*X*Y region, thus phosphorylation inhibits integrin activation by increasing the affinity of β integrin tails for a talin competitor that does not form activating membrane-proximal interactions with the integrin. Key residues governing these specificities were identified by detailed structural analysis, and talin1 was engineered to bind preferentially to phosphorylated integrins by introducing the mutation D372R. As predicted, this mutation affects talin1 localization in live cells in an integrin phosphorylation-specific manner. Together, these results indicate that tyrosine phosphorylation is a common mechanism for regulating integrin activation, despite subtle differences in how these integrins interact with their binding proteins.

Integrins play a fundamental role in cell adhesion and migration, linking the extracellular matrix to the actin cytoskeleton. In the adult, integrins are essential for a variety of biological processes including wound healing, leukocyte trafficking, and angiogenesis, and are thus increasingly attractive therapeutic targets for a variety of conditions, notably cancer. Mammals express 18 different α subunits and 8 different β subunits, which form 24 unique αβ heterodimers (excluding splice variants). Each α and β chain of the integrin heterodimer consists of several linked globular extracellular domains, a single membrane-spanning domain, and a short cytoplasmic tail (1). The cytoplasmic tails of the β subunits exhibit conserved regions (Fig. 1*A*), and act as a hub for protein-protein interactions (2), modulating a variety of signaling processes in both directions across the membrane. Extracellular adhesion can be activated from within the cell by the cytoskeletal protein talin (1, 3–5) via a direct interaction between the talin F3 domain and the membrane-proximal (MP)[3] portion of the integrin tail (6–8).

The different β integrins found in mammals occupy unique biological niches (1) and show significant diversity in their protein-protein interactions. Of the six β integrin tails that display a high level of sequence homology to one another (β1, β2, β3, β5, β6, and β7), all contain two NP*X*Y or NP*X*Y-like motifs, a near membrane-distal (nMD) site and a far membrane-distal (fMD) site, that bind to phosphotyrosine-binding (PTB) domains (including the talin F3 domain) (9) and are potential phosphorylation sites. In the β2 tail, however, both tyrosine residues are substituted with phenylalanine, and in the β7 tail this substitution occurs in the fMD site. Uniquely, the β7 tail also exhibits two additional MP tyrosine phosphorylation sites that are not part of an NP*X*Y motif (10).

This study explores three of these integrins: β3, β1A (the most common splice variant of β1), and β7 (see Fig. 1*A*). Previous studies on integrin tyrosine phosphorylation have generally focused on two of these: β3 and β1. When the β1 integrin was first isolated and sequenced, a potential tyrosine phosphorylation site was proposed (11), and an early study observed β1 tyrosine phosphorylation in response to transformation of cells with viral Src (v-Src) (12), followed by the demonstration of tyrosine phosphorylation of β1 by v-Src *in vitro* (13). These studies involved a viral protein, but it was later found that αIIbβ3 is tyrosine-phosphorylated in response to platelet acti-

* This work was supported, in whole or in part, by a National Institutes of Health grant (to M. H. G., I. D. C., and K. L. W.). This work was also supported by grants from the Wellcome Trust (to I. D. C. and C. L. O.) and the Rhodes Trust (to N. J. A.).

[S] The on-line version of this article (available at http://www.jbc.org) contains supplemental Figs. S1–S6.

The atomic coordinates and structure factors (code 3G9W) have been deposited in the Protein Data Bank, Research Collaboratory for Structural Bioinformatics, Rutgers University, New Brunswick, NJ (http://www.rcsb.org/).

[1] To whom correspondence may be addressed: Laboratory of Chemical Physics, Bldg. 5, National Institutes of Health, NIDDK, Bethesda, MD 20892-0520. E-mail: nick.anthis@gmail.com.

[2] To whom correspondence may be addressed: South Parks Road, Oxford OX1 3DR, United Kingdom. Tel.: 44-1865-613-200; Fax: 44-1865-613-201; E-mail: iain.campbell@bioch.ox.ac.uk.

[3] The abbreviations used are: MP, membrane-proximal; c-Src, cellular Src; fMD, far membrane-distal; HSQC, heteronuclear single quantum coherence; MEF, mouse embryonic fibroblast; nMD, near membrane-distal; NOESY, nuclear Overhauser enhancement spectroscopy; PTB, phosphotyrosine-binding; SYF, Src, Yes, and Fyn-deficient; TOCSY, total correlation spectroscopy; v-Src, viral Src; WT, wild type; GFP, green fluorescent protein.

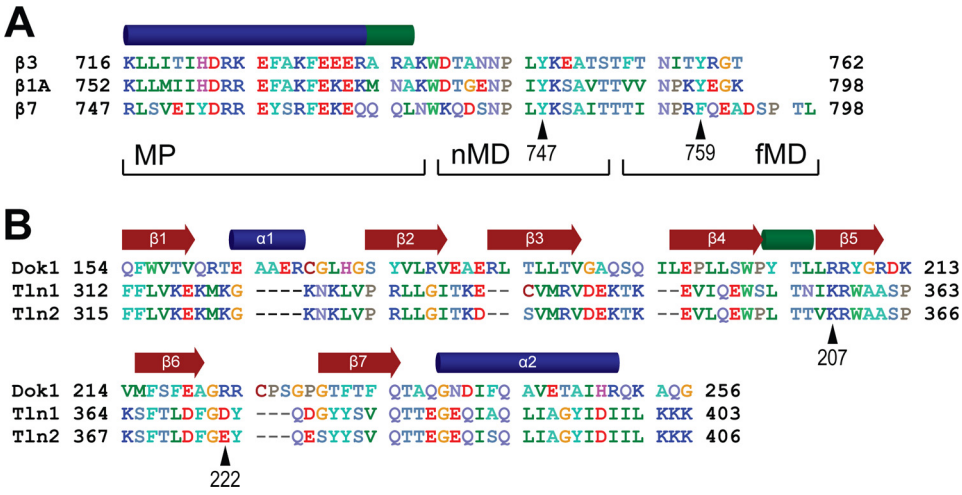

FIGURE 1. **Integrin tail and PTB domain sequence alignments.** *A,* sequences of the cytoplasmic regions of the β3, β1A, and β7 integrin tails. The two NPXY motif tyrosine residues are indicated, with β3 numbering. The MP, nMD, and fMD regions are denoted. Secondary structure is based on the β1D·talin2 complex structure (44), with α helices denoted in *blue* and 3_{10} helices in *green*. *B,* sequences of the PTB domains of Dok1, talin1, and talin2 aligned by secondary structure, with secondary structure elements from the Dok1 PTB domain structure (PDB 2V76) (43) shown. Notable residues are indicated with Dok1 numbering.

vation, and that cellular Src (c-Src) and related tyrosine kinases phosphorylate β3 *in vitro* (14). Studies suggest that β1 interacts with various Src family kinases and that these kinases are activated by integrin engagement with the extracellular matrix (15–22). There is also evidence for a direct and constitutive interaction between β3 and c-Src (23).

Various studies have demonstrated that tyrosine phosphorylation of β1 influences integrin localization and activity, as well as cell morphology. An early study showed that transformation of cells with Rous sarcoma virus, which expresses v-Src, leads to β1 integrins adopting a more diffuse distribution on the cell surface (12), rather than being localized in focal adhesions, which are large macromolecular complexes composed of integrins and intracellular proteins, such as vinculin, talin, and paxillin, which serve as sites of tight attachment to the extracellular matrix (24, 25). Transformed cells also display rounding, decreased fibronectin matrix assembly, and decreased cell migration (12). Another study found that whereas unphosphorylated β1 integrins localize to focal adhesions, phosphorylated integrins localize to podosomes (26).

Further insight has come from studies using non-phosphorylatable integrins with Tyr to Phe mutations (supplemental Fig. S1*A*). The Y783F mutation in the β1 nMD site reverses the effects of v-Src (27). Fibroblasts expressing β1 Y783F, Y795F, or Y783F/Y795F display impaired directed cell migration but increased fibronectin binding (28), and Y783F/Y795F also causes slowed cell spreading and decreased focal adhesion kinase activation (29). In β3, the nMD mutation Y747F disrupts adhesion and clot retraction in hematopoietic cells (30). More tellingly, mice with the knock-in double Y747F/Y759F mutation in β3 display a severe bleeding defect (31), although, surprisingly, mice with the analogous β1 knock-in mutation show no significant phenotype (32, 33).

The role of tyrosine phosphorylation in outside-in β3 signaling is relatively well established (30, 31, 34–41). The role in inside-out integrin activation is less clear, but various lines of evidence indicate that phosphorylation negatively regulates activation. Tyrosine phosphorylation of αVβ3 decreases the affinity of live cells for fibronectin (42), and phosphorylation of β1 decreases its affinity for fibronectin *in vitro* (13).

Dok1 is a signaling protein with a PTB domain capable of binding integrins (9). Dok1 negatively regulates β3 integrin activation (8), an observation initially difficult to explain due to the very weak interaction observed between these proteins. We subsequently reported that tyrosine phosphorylation greatly increases Dok1 affinity for short β3 peptides while slightly decreasing talin1 affinity, observations that led to an initial structural explanation for this phenomenon (Fig. 2) (43). However, these findings did not clarify the specific roles of the different NPXY motifs or indicate whether this mechanism could be generalized across different integrins. Here, we explore the phosphorylation dependence of the talin1 and Dok1 interactions with full-length β3, β1A, and β7 tails. We show that tyrosine phosphorylation is a common mechanism for regulating the affinity of these proteins for integrin tails, and a recent crystal structure of a talin·β1 complex (44) allows us to explain subtle differences between different integrins. We also describe the structural basis of this phosphorylation state specificity in detail and generate a talin mutant that shows preferential binding to phosphorylated integrin tails.

EXPERIMENTAL PROCEDURES

Expression and Purification of Proteins—Proteins and peptides were expressed in *Escherichia coli* and purified as reported previously (44), unless otherwise indicated. Integrin tail constructs corresponding to the entire predicted cytoplasmic region were produced in pET16b using the following boundaries: β3 Lys^{716}–Thr^{762}, β1A Lys^{752}–Lys^{798}, and β7 Arg^{747}–Leu^{798}. The talin1 F3 domain (Gly^{309}–Ser^{405}) and the Dok1 PTB domain (Gln^{154}–Gly^{256}) were produced in pGEX-6P-2 as reported previously (8). For experiments in mammalian cells, the cDNA encoding full-length mouse talin1 was amplified by PCR and subcloned into pEGFP-C1. Mutations in pET and pGEX vectors were introduced with the QuikChange kit, and mutations in pEGFP-C1 were introduced with the QuikChange II XL kit (Stratagene).

Cell Culture—SYF cells (mouse embryonic fibroblasts (MEFs) deficient in c-Src, c-Fyn, and c-Yes) and SYF + Src cells (SYF MEFs reconstituted with c-Src) (19) were obtained from the American Type Culture Collection. Cells were maintained in Dulbecco's modified Eagle's medium supplemented with 10% fetal bovine serum, L-glutamine, and antibiotics at 37 °C with 6% CO_2. Transient transfections were carried out with Lipofectamine Plus (Invitrogen) as described by the manufacturer.

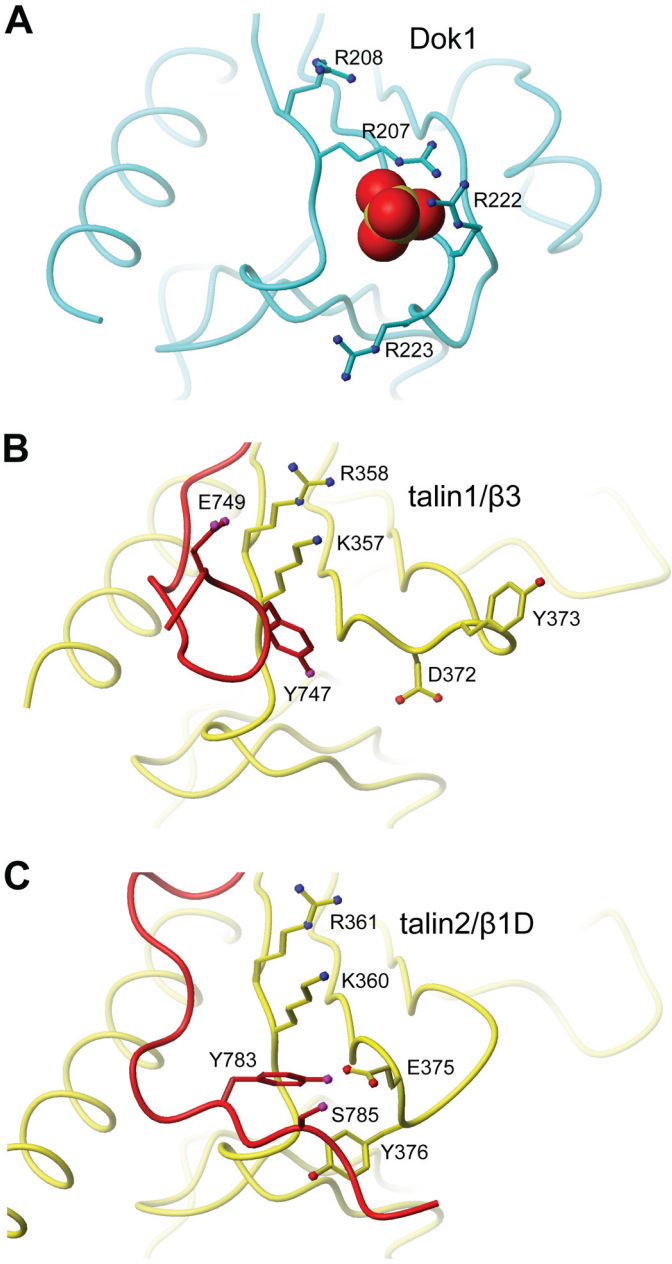

FIGURE 2. **The structural basis of Dok1 specificity for phosphorylated integrin tails.** *A*, detail of the Dok1 PTB domain structure (PDB 2V76) (43) showing a sulfate anion located in the NP*X*Y-binding pocket. Key positively charged residues are highlighted. *B*, detail of the NP*X*Y motif of the β3 integrin tail bound to the talin1 F3 domain (PDB 1MK9) (55). *C*, detail of the NP*X*Y motif of the β1D tail bound to the talin2 F3 domain (PDB 3G9W) (44). The residues highlighted in *panels B* and *C* are analogous to those highlighted in the Dok1 structure in *panel A*. Molecular images were generated with MOLMOL (61).

Tyrosine Phosphorylation of Integrin Tails—The kinase domain of c-Src (Gln^{251}–Leu^{533}) in pET28 was co-expressed with *Yersinia pseudotuberculosis* YopH in pCDFDuet-1 and purified by immobilized metal affinity chromatography as previously reported (45). Tyrosine phosphorylation was performed overnight at 30 °C with 20 μM integrin tail and 0.015 mg/ml of Src in 50 mM Tris, 20 mM $MgCl_2$, 10 mM $MnCl_2$, 1 mM ATP, 1 mM dithiothreitol, pH 7.0. Phosphorylated tails were separated from unphosphorylated tails by C_4 reverse phase high performance liquid chromatography and identified by mass spectrometry and NMR (supplemental Fig. S2). Preliminary experiments observed phosphorylation by autoradiography (supplemental Fig. S3).

NMR Spectroscopy—All NMR experiments were performed on spectrometers equipped with Oxford Instruments superconducting magnets (500, 600, 750, and 950 MHz ^1H operating frequencies) and GE/Omega computers. Unless otherwise indicated, samples were prepared in NMR buffer (50 mM sodium phosphate, 100 mM NaCl, 1 mM dithiothreitol, pH 6.1) with 5% D_2O and Complete protease inhibitors (Roche Applied Science). Experiments were performed at 25 °C. The ^1H and ^{15}N resonances of the ^{15}N-labeled β7 integrin tail were assigned using a 0.2 mM sample in 20 mM sodium acetate, pH 4.5, and employing three-dimensional NOESY-HSQC and three-dimensional TOCSY-HSQC spectra. Resonance assignments were transferred to pH 6.1 conditions through pH titrations. Spectra were referenced in the direct dimension to 2,2-dimethyl-2-silapentane-*S*-sulfonate at 0 ppm, with indirect referencing in the ^{15}N dimension using a $^{15}N/^1H$ frequency ratio of 0.101329118 (46). Data were processed using NMRPipe (47) and spectra were visualized using the program SPARKY or CCPN Analysis (48). The ^1H and ^{15}N resonance assignments of the β7 tail have been deposited in the Biological Magnetic Resonance Data Bank with accession number 16259. Resonances of β3 and β1A integrin tails were previously assigned and deposited under accession numbers 15552 (43) and 16159 (44), respectively.

Protein-Protein Interaction Studies—^1H-^{15}N HSQC titrations (supplemental Fig. S4) were performed with 0.05 mM ^{15}N-labeled integrin tail and increasing concentrations of unlabeled talin1 or Dok1, from 0 to 1 mM. Weighted combined ^1H and ^{15}N amide shifts (Δ(H,N)) were calculated using the equation,

$$\Delta(H,N) = \sqrt{\Delta_H W_H{}^2 + \Delta_N W_N{}^2} \qquad \text{(Eq. 1)}$$

where W_H and W_N are weighting factors for the ^1H and ^{15}N amide shifts, respectively ($W_H = 1$, $W_N = 0.154$) (49), and $\Delta = \delta_{bound} - \delta_{free}$. Dissociation constants were determined by fitting changes in backbone chemical shifts upon increasing talin concentration to the following equation,

$$\Delta(H,N) = \Delta(H,N)_{max}\frac{[L] + [U] + K_d - \sqrt{([L] + [U] + K_d)^2 - 4[L][U]}}{2[L]} \qquad \text{(Eq. 2)}$$

where K_d is the dissociation constant, $\Delta(H,N)$ is the weighted shift change, $\Delta(H,N)_{max}$ is the shift change at saturation, and $[L]$ and $[U]$ are the concentrations of the labeled and unlabeled proteins, respectively. Data from peaks that were well resolved, had a significant change in position, and were discernable throughout the titration were fit simultaneously to this equation with the program OriginPro 8, extracting a single K_d and multiple $\Delta(H,N)_{max}$ values. Values for ΔG were calculated from the K_d value.

Data are presented throughout as the K_d value ± S.E. This error only takes into account the uncertainty from the fitting

procedure. The other source of error in these experiments would be concentration errors, but they are not reported due to difficulty in estimating them. However, experience indicates that errors in K_d stemming from talin1 or Dok1 concentration determinations would at most be about 10% (corresponding to a maximum error in ΔG of 0.25 kJ/mol). For interactions with K_d values less than about 100 μM, this would be compounded by β integrin concentration determination errors, leading to a maximum total K_d error due to concentration errors of ~20% (corresponding to a maximum error in ΔG of 0.5 kJ/mol).

Some K_d values are reported as approximate because binding was too weak for the generation of a binding curve. In these cases, the value of $\Delta(H,N)_{max}$ was estimated by comparing maximum $\Delta(H,N)$ values for relevant peaks to the $\Delta(H,N)$ of peaks in a corresponding quantifiable titration. The fitting procedure was then carried out as before, but with the value of $\Delta(H,N)_{max}$ restrained. No errors are reported for these values, as they are only estimates.

Immunofluorescence Imaging—After transfection, MEF cells were plated on 7.5 μg/ml of fibronectin-coated coverslips, allowed to adhere for 90 min in Dulbecco's modified Eagle's medium, rinsed once in phosphate-buffered saline, and fixed with 3.7% formaldehyde in phosphate-buffered saline. After fixation, cells were permeabilized in 0.1% Triton X-100 for 5 min, blocked with 3% bovine serum albumin, 2% normal goat serum for 1 h, and then incubated with the appropriate primary antibody in blocking solution overnight at 4 °C. Bound antibodies were detected by the corresponding fluorescein isothiocyanate-conjugated goat secondary antibodies (Santa Cruz Biotechnology). Coverslips were subsequently mounted in Prolong Gold antifade reagent (Invitrogen) on slides. Epifluorescent images of cells were acquired with a ×60 oil immersion objective on a Nikon Eclipse TE2000-U microscope equipped with the appropriate excitation and emission filter sets (Semrock). Additional post-acquisition processing of images was performed using ImageJ (www.rsb.info.nih.gov/ij) and Adobe Photoshop.

Anti-green fluorescent protein (GFP) rabbit polyclonal antibody was obtained from Clontech. Anti-vinculin mouse monoclonal antibody was purchased from Sigma. Anti-phosphotyrosine (Tyr(P)[100]) mouse monoclonal antibody was purchased from Cell Signaling Technology. Anti-paxillin rabbit polyclonal antibody (RB4536) was developed in house.

RESULTS

Production of Tyrosine-phosphorylated Integrin Tails for NMR—Before the current study, structural work on integrin phosphorylation had involved short chemically synthesized integrin tail fragment peptides (43). However, we recently reported a robust system for studying integrin tail protein-protein interactions by NMR using full-length ^{15}N-labeled integrin tails produced in *E. coli*. This system is cost-effective and versatile, but using such a system to produce tyrosine-phosphorylated peptides presents additional difficulties; modified residues can be incorporated directly during chemical peptide synthesis, but not in *E. coli*. Although glutamate can be introduced by mutagenesis to make an acceptable mimic for phosphoserine or phosphothreonine, phosphotyrosine has no natural analogue (supplemental Fig. S1*B*). Thus, the integrin tails would have to be phosphorylated directly.

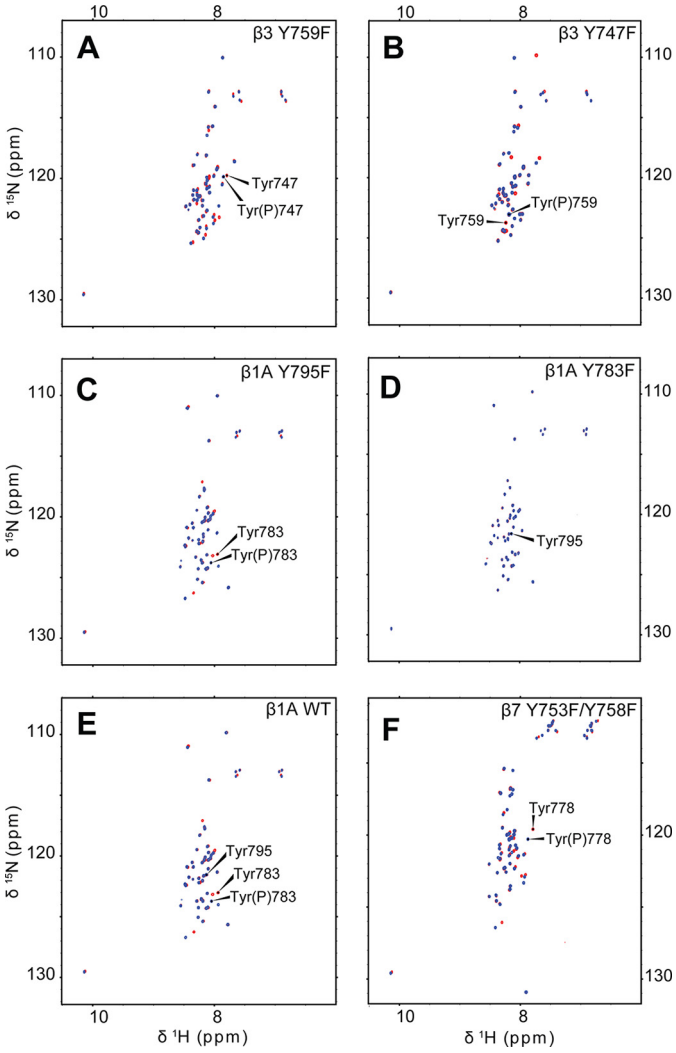

FIGURE 3. **Phosphorylation of integrin tails.** HSQC spectra of integrin tails before (*red*) and after (*blue*) the tyrosine phosphorylation reaction. Phosphorylated residues are indicated. *A*, β3 Y759F. *B*, β3 Y747F. *C*, β1A Y795F. *D*, β1A Y783F. *E*, β1A WT. *F*, β7 Y753F/Y758F.

After exploring other options (supplemental Fig. S2), we were able to produce NMR scale quantities of tyrosine-phosphorylated ^{15}N-labeled integrin tails by *in vitro* phosphorylation with c-Src, which has been used for *in vitro* phosphorylation of integrin tails in previous studies (14, 39), although not previously on a scale large enough for structural biology. Because tyrosine kinases can be toxic to bacteria, we produced the Src kinase domain in *E. coli* by coexpressing it with YopH phosphatase, as previously described by Seeliger *et al.* (45).

To phosphorylate specific tyrosine residues selectively, single and double Tyr to Phe mutants were made: β3 Y747F (for Tyr(P)[759]) and Y759F (for Tyr(P)[747]), β1A Y783F (for Tyr(P)[795]) and Tyr[795] (for Tyr(P)[783]), and β7 Y753F/Y758F (for Tyr(P)[778]). The β7 tail contains two MP tyrosine residues, but phosphorylation of just the nMD tyrosine residue was explored (the fMD site contains a natural Tyr to Phe substitution). Tyrosine phosphorylation caused localized perturbations in the HSQC spectra of the integrin tails (Fig. 3). Phosphorylation of

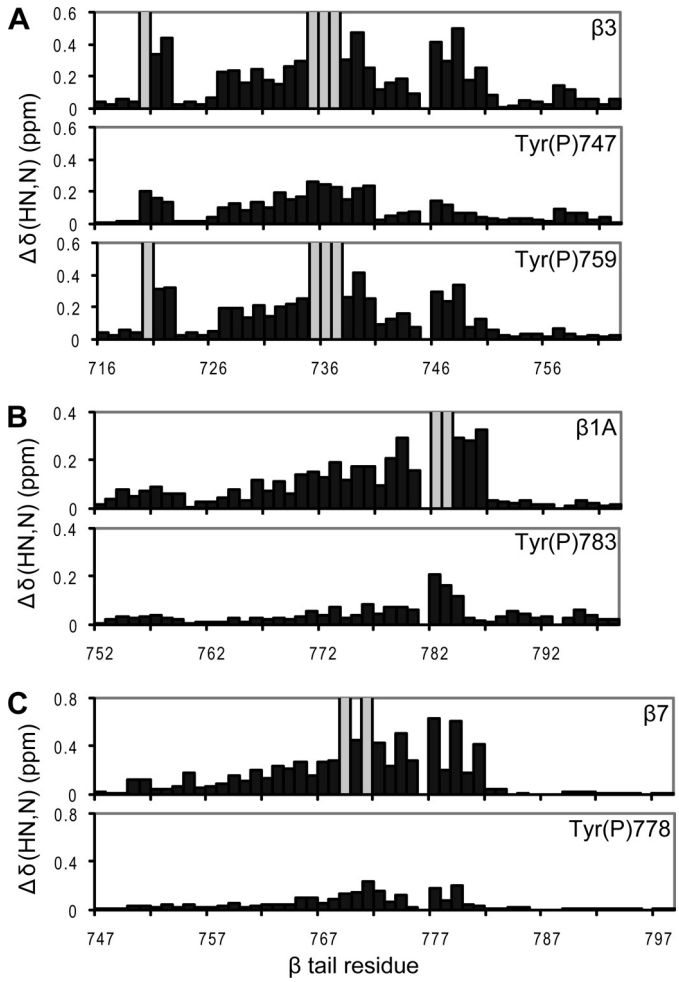

FIGURE 4. **Effect of tyrosine phosphorylation on the integrin/talin1 interaction.** Weighted chemical shift maps of perturbations observed in ^{1}H-^{15}N HSQC spectra of the β3 (*A*), β1A (*B*), and β7 (*C*) tails (50 μM) upon the addition of talin1 F3 domain (1 mM). Interaction studies were performed on unphosphorylated integrin tails and tails phosphorylated at the nMD site (β3, β1A, and β7) and at the fMD site (β3). *Gray bars* correspond to residues that could not be tracked due to exchange broadening. Note that the *y* axis scale differs between panels.

TABLE 1
Effect of tyrosine phosphorylation on the affinity of the integrin/talin1 interaction

Mutation	K_d[a]	ΔG[b]	$\Delta\Delta G_{pY}$[c]
	μM	kJ/mol	
β3			
WT	273 ± 6.4	−20.33 ± 0.06	
Y759F	286 ± 4.6	−20.22 ± 0.04	
Y759F Tyr(P)[747]	1032 ± 27	−17.04 ± 0.07	3.21
Y747F	366 ± 6.4	−19.61 ± 0.04	
Y747F Tyr(P)[759]	386 ± 15	−19.48 ± 0.10	0.13
β1A			
WT	491 ± 10	−18.88 ± 0.05	
Tyr(P)[783]	2,500 Est.[d]	−14.8	4.0
β7			
WT	142 ± 3.0	−21.95 ± 0.05	
Y753F/Y758F	145 ± 4.3	−21.89 ± 0.07	
Y753F/Y758F Tyr(P)[778]	1,217 ± 62	−16.63 ± 0.13	5.26

[a] K_d values are given ± S.E.
[b] ΔG is given for binding and calculated from K_d.
[c] $\Delta\Delta G_{pY}$ is the ΔG value for the phosphorylated integrin binding to talin1, minus the ΔG value for the unphosphorylated integrin binding to talin1 (a positive value denotes a decrease in affinity upon phosphorylation) (pY, Tyr(P)).
[d] Approximate K_d values were estimated by comparing the magnitude of chemical shift perturbations to those in a relevant titration, as described under "Experimental Procedures."

both β3 Y747F and Y759F was observed, as was phosphorylation of β1A Y795F and β7 Y753F/Y758F. However, phosphorylation of β1A Y783F was not observed. When the phosphorylation reaction was performed on β1A wild type (WT), chemical shift perturbations were only observed near Tyr^{783}, indicating that Tyr^{783}, but not Tyr^{795}, was phosphorylated in this system. Thus, for further studies, β1A $Tyr(P)^{783}$ was produced from WT peptides.

Tyrosine Phosphorylation Decreases Integrin Affinity for Talin—Binding of proteins to integrin tails was assayed by observing chemical shift perturbations in integrin tail HSQC spectra. Upon the addition of the talin1 F3 domain to the β3, β1A, or β7 tails, significant perturbations were observed in the MP and nMD portions of the tail (Fig. 4). The MP perturbations were greatest in the β3 tail, but they were present in all tails tested. The affinities of these interactions were quantified, giving K_d values that ranged from 142 μM for β7 to 273 μM for β3 to 491 μM for β1A (Table 1). Smaller shifts were also observed in the fMD portion of the β3 integrin tail (and to a lesser extent in the β1A tail), but these perturbations are likely due to a weak competing integrin/talin interaction, with a K_d of several millimolar for the fMD portion.

The introduction of Tyr to Phe mutations employed for specific phosphorylation in β3 and β7 had negligible effects on talin affinity in these integrins. The greatest effect was seen with Y747F in β3, which increased the K_d to 366 μM (see Table 1). Such a decrease in affinity upon a mutation in the talin-binding site is not surprising, and it is notable that this effect is very small compared with the much greater changes in affinity observed elsewhere in this study.

Tyrosine phosphorylation of the nMD NP*X*Y motif decreased the magnitude of chemical shift perturbations observed upon talin binding (Fig. 4) and decreased the affinity of these interactions. This effect was most pronounced in β7, less so in β1A, and least in β3. Phosphorylation of the fMD NP*X*Y motif in β3 abrogated chemical shift perturbations upon talin binding in that region, but had little effect on the much tighter interaction with the MP and nMD regions or the overall affinity (see Table 1).

Tyrosine Phosphorylation Increases Integrin Affinity for Dok1—Unlike the talin1 F3 domain, the PTB domain of Dok1 only caused small perturbations in the HSQC spectra of unphosphorylated integrin tails. Such perturbations were localized to the nMD region of β3 and the fMD regions of β1A and β7 (supplemental Fig. S5). However, these interactions were so weak (K_d greater than several millimolar) that it is unlikely that any of these interactions are physiologically relevant (Table 2). It is of note that although the K_d value for β3 (12.6 mM) is only an estimate, as described under "Experimental Procedures," it agrees well with the 14.3 mM value reported for a short fragment of β3 (43).

Upon phosphorylation, the affinities of these interactions increased substantially. For phosphorylation in the nMD regions, K_d values ranged from 20.9 μM for β3 to 36.8 μM for β7 to 78.7 μM for β1A (see Table 2 and supplemental Fig. S4). Phosphorylation of β3 Tyr^{759} also increased Dok1 affinity to a K_d of 226 μM. In each case, the interaction as observed by NMR

TABLE 2
Effect of tyrosine phosphorylation on the affinity of the integrin/Dok1 interaction

Mutation	K_d[a]	ΔG[b]	$\Delta\Delta G_{pY}$[c]
	μM	kJ/mol	
β3			
WT	12,600 Est.[d]	−10.8	
Y759F Tyr(P)[747]	20.9 ± 2.9	−26.69 ± 0.34	−15.9
Y747F Tyr(P)[759]	226 ± 7.7	−20.80 ± 0.08	−10.0
β1A			
WT	N/A[e]		
Tyr(P)[783]	78.7 ± 2.4	−23.41 ± 0.07	
β7			
WT	N/A		
Y753F/Y758F Tyr(P)[778]	36.8 ± 1.4	−25.30 ± 0.09	

[a] K_d values are given ± S.E.
[b] ΔG is given for binding and calculated from K_d.
[c] $\Delta\Delta G_{pY}$ is the ΔG value for the phosphorylated integrin binding to Dok1, minus the ΔG value for the unphosphorylated integrin binding to Dok1 (a negative value denotes an increase in affinity upon phosphorylation) (pY, Tyr(P)).
[d] Approximate K_d values were estimated by comparing magnitude of chemical shift perturbations to those in a relevant titration, as described under "Experimental Procedures."
[e] No detectable binding to the applicable binding site.

was localized to residues near the site of phosphorylation. No MP perturbations were observed in β3 or β1A, and only minor MP perturbations in β7 (Fig. 5). Tyrosine phosphorylation thus greatly increases the affinity of Dok1 for integrin tails (adding 16 kJ/mol of binding energy to the interaction in the case of β3 Tyr(P)[747]), making the interaction tight enough to be physiologically relevant and significantly tighter than the competing talin/integrin interaction.

Experiments were also conducted on a β3 Y747E mutant. Glutamate is occasionally reported as a phosphotyrosine mimic, despite very little chemical similarity to phosphotyrosine (supplemental Fig. S1*B*). The chemical shift perturbation pattern of this mutant upon interaction with Dok1 closely resembled that of β3 Y747A (supplemental Fig. S6). In both cases, interaction with the nMD NP*X*Y region was abrogated. This stands in stark contrast to the significant increase in chemical shift perturbations observed upon phosphorylation of Tyr[747]; this strongly suggests that glutamate is an unwise choice as a phosphotyrosine mimic.

Positively Charged Residues in the NPXY-binding Pocket Make Dok1 Specific for Phosphorylated Integrin Tails—When we solved the crystal structure of the human Dok1 PTB domain (Protein Data Bank 2V76) (43), we found a sulfate anion in the NP*X*Y-binding pocket, surrounded by a collection of positively charged residues: Arg[207], Arg[208], Arg[222], and Arg[223]. Arg[207] and Arg[222] make the most direct contact (Fig. 2*A*). We hypothesized that these positively charged residues may explain the higher affinity of Dok1 for phosphorylated β3; we tested this hypothesis by individually mutating these residues to alanine. These mutations only had minor effects on the affinity of Dok1 for unphosphorylated β3 tail, but the effect was much more pronounced on the interaction with β3 tail phosphorylated at Tyr[747] (Table 3). R207A had the greatest effect (increasing the K_d of the interaction with phosphorylated β3 from 20.9 to 1,485 μM), followed by R222A (increasing the K_d to 398 μM).

The degree to which each residue contributes to Dok1 phosphotyrosine specificity was calculated by subtracting the change in ΔG caused by the Arg to Ala mutation for the interaction with the unphosphorylated tail from the change in ΔG for the interaction with the phosphorylated tail (yielding the value $\Delta\Delta G_{RA/pY}$ in Table 3); the additive loss of phosphotyrosine-specific affinity for all four mutations (20.8 kJ/mol) is more than enough to explain the 15.9 kJ/mol increase in binding affinity of Dok1 upon β3 phosphorylation at Tyr[747]. Arg[207] and Arg[222] are the greatest contributors to phosphotyrosine specificity (44 and 30%, respectively), but Arg[223] and Arg[208] also play a role (17 and 9%, respectively).

Residues Arg[207] and Arg[208] correspond to positively charged residues in talin, but Arg[222] and Arg[223] do not. Residue Arg[223] corresponds to Tyr[373] in talin1 and Tyr[376] in talin2, a residue that plays a significant role in binding integrins, particularly β1 integrins.[4] Interestingly, however, Arg[222] corresponds to a negatively charged residue (Asp[372] in talin1 and Glu[375] in talin2, see Fig. 2). Thus, Arg[222] was chosen as a particularly suitable candidate for exploring differences in specificity for phosphorylated integrin tails between Dok1 and talin.

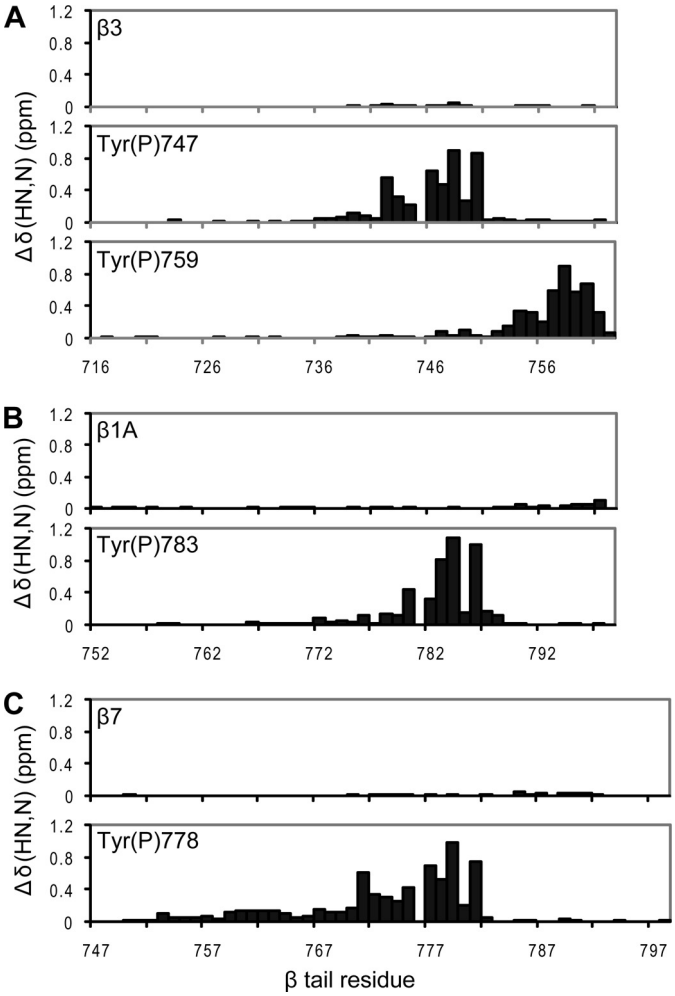

FIGURE 5. **Effect of tyrosine phosphorylation on the integrin/Dok1 interaction.** Weighted chemical shift maps of perturbations observed in ^{1}H-^{15}N HSQC spectra of the β3 (*A*), β1A (*B*), and β7 (*C*) tails (50 μM) upon the addition of the Dok1 PTB domain (1 mM). Interaction studies were performed on unphosphorylated integrin tails and tails phosphorylated at the nMD site (β3, β1A, and β7) and at the fMD site (β3).

[4] N. J. Anthis, H. B. Schiller, K. L. Wegener, A. Raducanu, D. R. Critchley, R. Fässler, and I. D. Campbell, manuscript in preparation.

TABLE 3
Disrupting Dok1 binding to phosphorylated β integrin tails

Mutation	K_d[a]	ΔG[b]	$\Delta\Delta G_{RA}$[c]	$\Delta\Delta G_{pY}$[d]	$\Delta\Delta G_{RA/pY}$[e]	$\Delta\Delta G_{RA/pY}$[f]
	μM		kJ/mol			%
β3 WT						
Dok1 WT	12,600 Est.[g]	−10.8				
Dok1 R207A	22,800 Est.	−9.4	1.5			
Dok1 R208A	22,600 Est.	−9.4	1.4			
Dok1 R222A	18,600 Est.	−9.9	1.0			
Dok1 R223A	13,900 Est.	−10.6	0.2			
β3 Y759F Tyr(P)^{747}						
Dok1 WT	20.9 ± 2.87	−26.69 ± 0.34		−15.9		
Dok1 R207A	1,485 ± 64	−16.14 ± 0.11	10.56	−6.8	9.1	44
Dok1 R208A	77.3 ± 1.3	−23.46 ± 0.04	3.24	−14.1	1.8	9
Dok1 R222A	398 ± 18	−19.40 ± 0.11	7.30	−9.5	6.3	30
Dok1 R223A	101 ± 3.3	−22.80 ± 0.08	3.89	−12.2	3.6	17

[a] K_d values are given ± S.E.
[b] ΔG is given for binding and calculated from K_d.
[c] $\Delta\Delta G_{RA}$ (kJ/mol) is the ΔG value for the integrin binding to mutant Dok1, minus the ΔG value for binding to Dok1 WT (a positive value denotes a decrease in affinity upon mutation).
[d] $\Delta\Delta G_{pY}$ (kJ/mol) is the ΔG value for the phosphorylated integrin binding to Dok1, minus the ΔG value for the unphosphorylated integrin binding to Dok1 (a negative value denotes an increase in affinity upon phosphorylation) (pY, Tyr(P)).
[e] $\Delta\Delta G_{RA/pY}$ (kJ/mol) is the $\Delta\Delta G_{pY}$ value for the integrin binding to mutant Dok1, minus the $\Delta\Delta G_{pY}$ value for binding to Dok1 WT.
[f] $\Delta\Delta G_{mut}$ (%) is the percentage of phosphorylated integrin-specific binding energy lost by the given mutation.
[g] Approximate K_d values were estimated by comparing magnitude of chemical shift perturbations to those in a relevant titration, as described under "Experimental Procedures."

TABLE 4
Engineering talin1 to preferentially bind to phosphorylated integrin tails

Mutation	K_d[a]	ΔG[b]	$\Delta\Delta G_{DR}$[c]	$\Delta\Delta G_{pY}$[d]
	μM	kJ/mol		
β3 + talin1 F3 D372R				
WT	86 ± 3.3	−23.18 ± 0.09	−2.85	
Y759F Tyr(P)^{747}	33.1 ± 1.6	−25.56 ± 0.12	−8.52	−2.38
β1A + talin1 F3 D372R				
WT	793 ± 24	−17.69 ± 0.07	1.19	
Tyr(P)^{783}	128 ± 5.1	−22.21 ± 0.10	−7.4	−4.52

[a] K_d values are given ± S.E.
[b] ΔG is given for binding and calculated from K_d.
[c] $\Delta\Delta G_{DR}$ is the ΔG value for integrin binding to talin1 D372R, minus the ΔG value for binding to talin1 WT (a negative value denotes an increase in affinity upon mutation).
[d] $\Delta\Delta G_{pY}$ is the ΔG value for the phosphorylated integrin binding to talin1, minus the ΔG value for the unphosphorylated integrin binding to talin1 (a negative value denotes an increase in affinity upon phosphorylation) (pY, Tyr(P)).

Engineering Talin to Bind Preferentially to Phosphorylated Integrin Tails—As discussed above, Dok1 Arg^{222} has a reversed charge in talin (Asp^{372} in talin1 and Glu^{375} in talin2) and is a key residue for determining Dok1 specificity for phosphorylated integrins. Consistent with this, introduction of the mutation D372R in talin1 substantially increased its binding affinity for integrin tails phosphorylated at the nMD site: 33.1 μM for β3 Tyr(P)^{747} and 128 μM for β1A Tyr(P)^{783} (Table 4).

Interestingly, this mutation also affected talin1 binding to unphosphorylated integrin tails in different ways, although to a lesser degree. Talin1 D372R binds more tightly to unphosphorylated β3 than does talin1 WT (86 *versus* 273 μM), but binds more weakly to unphosphorylated β1A than talin1 WT (793 *versus* 491 μM). These differences can be explained based on recent structural data (see Fig. 2) and could influence the biological activity of this mutant.

Talin D372R Localizes to Phosphorylated Integrins in Live Cells—Due to its dramatic effect on talin binding to phosphorylated integrins, we hypothesized that the D372R mutation would affect talin activity *in vivo*; we investigated this by examining talin localization to focal adhesions. We transiently expressed GFP-talin1 WT or D372R in SYF MEFs (deficient for the tyrosine kinases Src, Yes, and Fyn), which were then plated on fibronectin (an extracellular ligand for α5β1) and stained for the focal adhesion marker vinculin. Talin1 D372R was abundantly expressed (Fig. 6*D*) but was not seen at the sites of focal adhesions, whereas talin1 WT co-localized with vinculin and was therefore present in focal adhesions (Fig. 6*A*). Focal adhesions were also more prominent in cells expressing talin1 WT compared with those expressing talin1 D372R.

In SYF MEFs stably reconstituted with c-Src (SYF + Src), talin1 WT was also targeted to focal adhesions, but these adhesions were less prominent than in cases where c-Src was absent (Fig. 6*B*). However, talin1 D372R in SYF + Src MEFs was targeted to focal adhesions, and these were more prominent than those observed in SYF MEFs expressing talin1 D372R or SYF + Src MEFs expressing talin1 WT. To confirm the levels of phosphorylation in SYF MEFs and SYF + Src MEFs, fixed cells were stained with an anti-phosphotyrosine antibody (Tyr(P)^{100}), and an anti-paxillin antibody to mark focal adhesions (Fig. 6*C*). Greater phosphorylation was observed in the focal adhesions of SYF + Src MEFs when compared with SYF MEFs. In agreement with our structural model, these data suggest that talin1 D372R is capable of competing with endogenous talin for integrin binding only when integrins are tyrosine phosphorylated. Furthermore, tyrosine phosphorylation appears to affect cell morphology in a manner that is reversed by the D372R mutation.

DISCUSSION

Here, we have demonstrated that key interactions involving the β3, β1A, and β7 integrin cytoplasmic tails are similarly affected by tyrosine phosphorylation. Phosphorylation at the nMD site in each tail decreases its affinity for talin; in contrast, phosphorylation greatly increases the affinity for Dok1 (by 15.9 kJ/mol in the case of β3). The interaction of Dok1 is localized to the NP*X*Y region of the integrin tail, even when the affinity is relatively high (20.9 μM for β3 Tyr(P)^{747}). Talin, on the other hand, also binds to the MP region, a unique interaction that is essential for integrin activation (8). Thus, tyrosine phosphorylation acts to decrease integrin activation both by decreasing

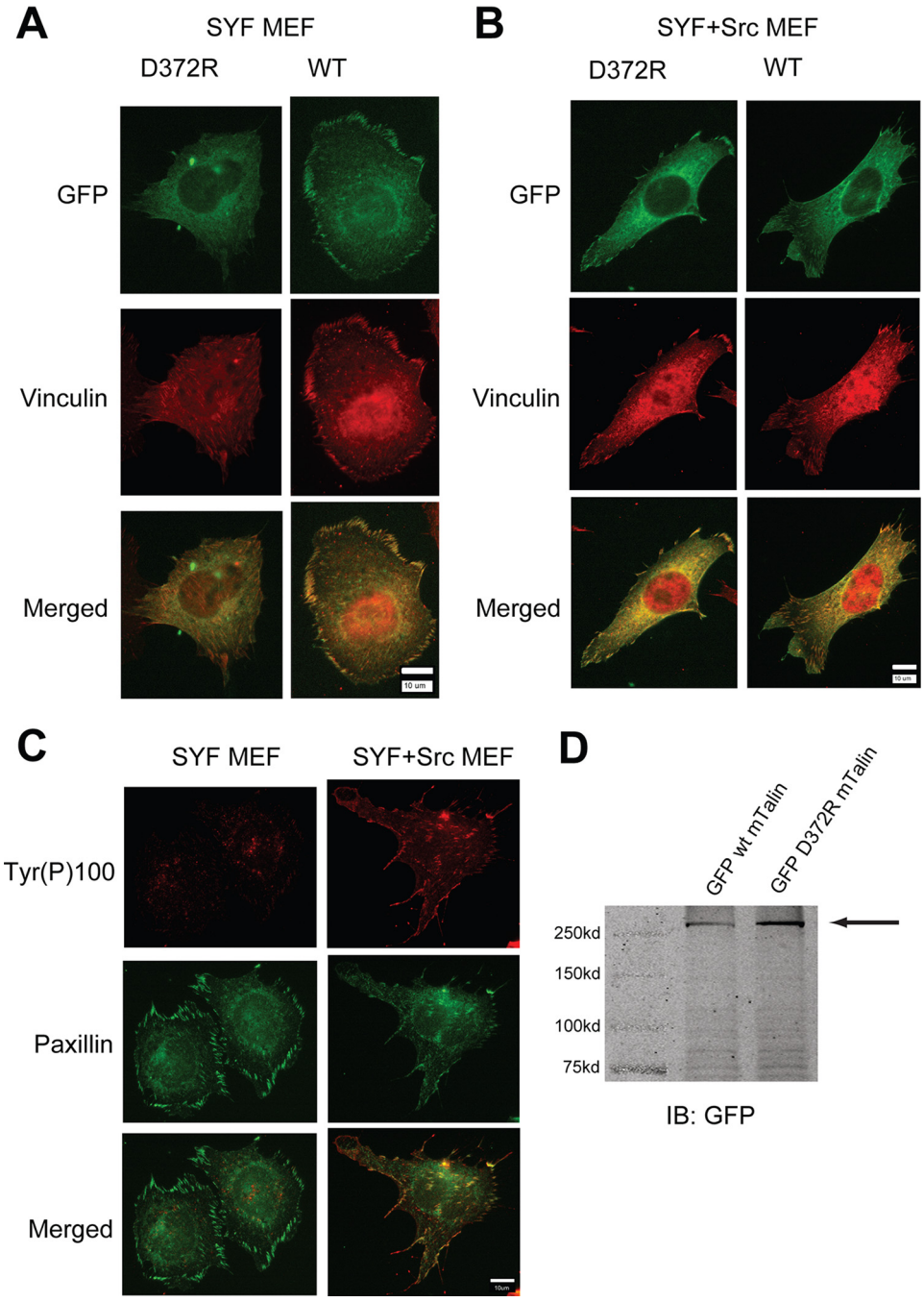

FIGURE 6. **Talin D372R preferentially localizes to focal adhesions that are tyrosine phosphorylated.** *A*, SYF MEFs and *B*, SYF + Src MEFs transiently expressing GFP-talin1 WT or D372R were allowed to adhere to fibronectin-coated coverslips and stained to visualize vinculin. Depicted are the localization of talin (*green*) and vinculin (*red*). *C*, SYF MEFs and SYF + Src MEFs were stained to visualize phosphotyrosine (Tyr(P)^{100}, *red*) and paxillin (*green*). *D*, SYF cells expressing GFP-talin1 and GFP-talin1 D372R were lysed and analyzed by Western blotting to confirm comparable expression of D372R and WT talin1.

talin affinity and increasing the affinity of competing proteins incapable of activating the integrin. This is consistent with our recent reports on β3 (43) and an early report on β1 (13), although our current report is the first detailed analysis of tyrosine phosphorylation across different integrins using structural biological methods.

By performing these studies on intact full-length integrin tails, we have been able to show definitively where these interactions are localized within the cytoplasmic tails, and we can look at the effect of independently phosphorylating different tyrosine residues within the same peptide. In β3, we could phosphorylate either Tyr^{747} or Tyr^{759}; in either case, the interaction with Dok1 was localized only to the site of phosphorylation. Whereas phosphorylation at Tyr^{747} disrupted the interaction with talin, phosphorylation at Tyr^{759} did not. Thus, the role of phosphorylation at this fMD site is probably not related to integrin activation; the integrin tail is very flexible in this region (50), and binding of Dok1 here would not be expected to compete with talin binding. The effect of phosphorylation on Dok1 binding was an order of magnitude higher at the Tyr^{747} site in β3, also demonstrating that the nMD site may play a more central role in Dok1 signaling.

This is the first publication of the talin-induced chemical shift perturbation map for β7, a lymphocyte-specific integrin (51), expanding our studies performed on β3 and β1A (44). Although showing some subtle differences to the interaction of talin with β3 and β1A, the interaction with β7 is broadly similar in that it consists of both MP and nMD interactions. In fact, the chemical shift perturbation map appears intermediate between those of β3 and β1A. In studying talin binding, it was found to be particularly important to use full-length peptides, given the large interaction surface. For example, in our previous study we reported the K_d of the interaction between talin and a short β3 peptide to be 3.49 (unphosphorylated) and 6.53 mM (phosphorylated) (43), whereas the values for the full-length β3 peptide reported here are, respectively, 0.273 and 1.03 mM. With respect to Dok1, which engages a more limited interaction surface, the values are more comparable between truncated and full-length tails.

These experiments could only be carried out on phosphorylated integrin tails, as a suitable phosphomimetic mutation does not exist for studying tyrosine phosphorylation. In fact, we show here that mutating Tyr^{747} in β3 to glutamate has the same effect as mutating that residue to alanine, which effectively abrogates protein-protein interactions in that region

(supplemental Fig. S6). This is observed for interactions with Dok1 and talin1, but in the case of Dok1 phosphorylation of Tyr^{747} strongly enhances binding, demonstrating that in this system at least, glutamate does not mimic phosphotyrosine. Any use of glutamate or aspartate as a phosphotyrosine mimic should therefore be extensively validated, at the very least by comparing it to the effect of an alanine substitution. The results of a rudimentary search through recent literature suggest that this is not common practice, and recent studies that did compare a "phosphomimetic" Tyr to Glu (or Tyr to Asp) mutant with a Tyr to Ala mutant found that the two different mutations had the same effect on the system under study (52, 53), meaning that the observed effects cannot necessarily be interpreted as being phosphorylation specific. This should not be a surprising result, given the lack of structural similarity between glutamate and phosphotyrosine (Fig. 1*B*).

Here, we show that mutation of positively charged residues in the NP*X*Y-binding pocket of Dok1 (Fig. 2*A*) (43) disrupts Dok1 binding to the β3 integrin tail in a phosphorylation-specific manner. It has been reported that the mutation of two of these residues to alanine (R207A/R208A) decreases Dok1 binding to β3 and disrupts Dok1 signaling (54). We can now explain this observation in terms of interference with the positively charged pocket necessary for specific binding of phosphorylated integrins, particularly Arg^{207}, which explains 44% of Dok1 phosphotyrosine specificity (Table 3). The analogous residues in talin1 and talin2, however, are also positively charged, so this does not explain why Dok1 binds specifically to phosphorylated integrins, whereas talin does not. Another residue in the Dok1 NP*X*Y-binding pocket, Arg^{222}, is oppositely charged in talin (Asp^{372} in talin1 and Glu^{375} in talin2). Mutation of this residue in Dok1 to alanine significantly decreases the affinity of the interaction with the β3 integrin in a phosphorylation-dependent manner, and is the largest contributor to Dok1 phosphotyrosine specificity after Arg^{207}.

We hypothesized that this understanding of the structural basis of the phosphorylation dependence of Dok1 could be used to engineer a talin variant that would bind specifically to phosphorylated integrins. Indeed, this effect was observed for talin1 D372R. This mutation increased talin affinity for phosphorylated β3 by 8.5 kJ/mol and β1A by 7.4 kJ/mol. Interestingly, this mutant had differing effects on the interaction with unphosphorylated integrins: it increased talin1 affinity for unphosphorylated β3 by 2.9 kJ/mol but decreased affinity for β1A by 1.2 kJ/mol. An examination of the structures of β3 and β1D in complex with talin (see Fig. 2) explains this difference. In the β3/talin1 structure (PDB 1MK9) (55), the portion of the tail C-terminal to Tyr^{747} does not make extensive contacts with talin. However, this region contains a negatively charged glutamate residue (Glu^{749}) that could make favorable electrostatic contacts with the mutant D372R. β1A, on the other hand, has an uncharged serine residue (Ser^{785}) in this position. In the β1D/talin2 structure (PDB 3G9W) (44), Ser^{785} forms a hydrogen bond with talin2 Glu^{375}. In the similar β1A·talin1 complex this mutation would disrupt such an interaction if present and would not be expected to make the interaction more favorable as in the case of β3. This interaction between the β1 Tyr^{783} side chain and a negatively charged talin residue may also explain why the introduction of a phosphate group here has a slightly greater disruptive effect on the β1A/talin1 interaction than on the β3/talin1 interaction (see Table 1). In addition, the Glu^{749}-Ser^{785} substitution may explain why Dok1 has a higher affinity for β3 than for β1A or β7 (which also has an uncharged residue, Ser^{780}, at this position), as Glu^{749} in β3 would form favorable electrostatic interactions with the positively charged Dok1-binding pocket.

We tested aspects of our structural model by observing the behavior of talin1 WT and D372R in live cells. In MEFs that do not express Src or related kinases, talin1 WT localized to focal adhesions, but talin1 D372R did not. As these experiments were carried out using fibronectin, and α5β1 is the primary fibronectin receptor in MEFs (56), this effect correlates with the decreased affinity observed between mutant talin and unphosphorylated β1A integrins. When c-Src was introduced into these cells, both talin1 WT and D372R co-localized with phosphorylated integrins at focal adhesions. Thus, the effects observed in *in vitro* binding experiments translate into observable effects in live cells. Interestingly, tyrosine phosphorylation correlates with reduced focal adhesion formation in the presence of talin1 WT but not talin1 D372R. We did not assess integrin inside-out activation levels directly, but the increased prominence of focal adhesions in c-Src-expressing cells in the presence of talin1 D372R *versus* talin1 WT provides evidence that this talin mutant disrupts the integrin activation phosphorylation switch, causing integrins to remain active even after integrin tyrosine phosphorylation. Thus, these results provide additional evidence that integrin tyrosine phosphorylation down-regulates integrin activation by inhibiting talin binding.

Phosphorylation of the nMD tyrosine residue has been shown to modulate inside-out integrin activation in β3 (42) and in β1 (13). In β3, phosphorylation of both nMD Tyr^{747} (30, 31, 34–36) and fMD Tyr^{759} (38, 39, 41) have been associated with outside-in signaling. This is consistent with a report that the nMD region of β3 in general is associated with both inside-out and outside-in signaling, whereas the fMD portion primarily engages only in outside-in signaling (57). This makes sense from a structural standpoint, in that talin only interacts tightly with the nMD NP*X*Y. For β1, studies point to a role for phosphorylation at nMD Tyr^{783} in signaling in both directions. Evidence for a signaling role for Tyr^{795} phosphorylation is sparser, but also exists (28, 29). However, under the conditions used in this study, c-Src did not phosphorylate this residue, so a different kinase may be involved *in vivo*. Interestingly, in β7 this fMD residue is a non-phosphorylatable phenylalanine.

Despite the substantial evidence for a role for tyrosine phosphorylation in β1 integrin signaling, mice with the β1 Y783F/Y795F knock-in mutation do not display any apparent developmental abnormalities (32, 33). The β3 Y747F/Y759F mouse, however, displays a severe phenotype (31). β1 tyrosine phosphorylation is central to the pathological effect of v-Src on cells (12, 26, 27), but given that these residues are so highly conserved across different integrins and across different species, it is unlikely that such conservation would exist if the residue only participated in pathological conditions. In the case of β3, at least, mutation of either NP*X*Y tyrosine to phenylalanine had

little effect on the interaction with talin1, so it is reasonable to hypothesize that these residues are conserved as tyrosine because of a role for phosphorylation, although the side chains of unphosphorylated β1D^4 Tyr^{783} and β3 Tyr^{747} (55) do also participate in intermolecular hydrogen bonds in complex with talin. The β1 Y783F/Y795F mutation affects cell behavior in tissue culture conditions (28, 29), so the lack of a phenotype in β1 Y783F/Y795F knock-in mice may be the result of compensation by other integrins. On the other hand, the more extreme effect of tyrosine phosphorylation on Dok1 binding to β3 correlates with the more definitive biological role observed for tyrosine phosphorylation in that integrin.

Several studies have provided evidence for a biological role for a direct interaction between Dok1 and β3 integrins (8, 54, 58, 59), but what role Dok1 plays in the signaling of other integrins remains more of an open question. A variety of other PTB domains have been identified that also interact with integrins (9), and it is possible that one of these other proteins acts as a phosphorylation-dependent activation switch for β1 or other integrins. The PTB domain of integrin cytoplasmic domain-associated protein 1 (ICAP-1), for example, has been identified as a phosphorylation-independent down-regulator of β1 activation, but given the large number of PTB domains that bind preferentially to phosphorylated substrates (60), other phosphorylation-dependent down-regulators may also exist. Given this uncertainty, however, and the results of the β1 Y783F/Y795F knock-in mouse (32, 33), this is an area that will require further study.

From the current study, and from the bulk of structural and biological data on the topic, integrin tyrosine phosphorylation appears to be involved in a wide variety of integrin signaling processes, particularly for β3, but for other integrins as well. We demonstrate here a conserved structural mechanism in β3, β1A, and β7 integrins for regulation of integrin activation by nMD tyrosine phosphorylation. We have tested our predictions by engineering a talin mutant that is specific for phosphorylated integrins, and we have shown that this influences talin localization in live cells. Given that the literature on integrin tyrosine phosphorylation is substantial but sometimes ambiguous, our results add weight to the idea that tyrosine phosphorylation plays a significant role in integrin signaling.

Acknowledgments—We thank Markus Seeliger and John Kuriyan for kindly supplying Src and YopH constructs, Max Soegaard for assistance with in vitro phosphorylation, and Ioannis Vakonakis for assistance with NMR experiments.

REFERENCES

1. Hynes, R. O. (2002) *Cell* **110,** 673–687
2. Liu, S., Calderwood, D. A., and Ginsberg, M. H. (2000) *J. Cell Sci.* **113,** 3563–3571
3. Ginsberg, M. H., Partridge, A., and Shattil, S. J. (2005) *Curr. Opin. Cell Biol.* **17,** 509–516
4. Campbell, I. D., and Ginsberg, M. H. (2004) *Trends Biochem. Sci.* **29,** 429–435
5. Calderwood, D. A. (2004) *J. Cell Sci.* **117,** 657–666
6. Calderwood, D. A., Yan, B., de Pereda, J. M., Alvarez, B. G., Fujioka, Y., Liddington, R. C., and Ginsberg, M. H. (2002) *J. Biol. Chem.* **277,** 21749–21758
7. Tadokoro, S., Shattil, S. J., Eto, K., Tai, V., Liddington, R. C., de Pereda, J. M., Ginsberg, M. H., and Calderwood, D. A. (2003) *Science* **302,** 103–106
8. Wegener, K. L., Partridge, A. W., Han, J., Pickford, A. R., Liddington, R. C., Ginsberg, M. H., and Campbell, I. D. (2007) *Cell* **128,** 171–182
9. Calderwood, D. A., Fujioka, Y., de Pereda, J. M., García-Alvarez, B., Nakamoto, T., Margolis, B., McGlade, C. J., Liddington, R. C., and Ginsberg, M. H. (2003) *Proc. Natl. Acad. Sci. U.S.A.* **100,** 2272–2277
10. Krissansen, G. W., Singh, J., Kanwar, R. K., Chan, Y. C., Leung, E., Lehnert, K. B., Kanwar, J. R., and Yang, Y. (2006) *Eur. J. Immunol.* **36,** 2203–2214
11. Tamkun, J. W., DeSimone, D. W., Fonda, D., Patel, R. S., Buck, C., Horwitz, A. F., and Hynes, R. O. (1986) *Cell* **46,** 271–282
12. Hirst, R., Horwitz, A., Buck, C., and Rohrschneider, L. (1986) *Proc. Natl. Acad. Sci. U.S.A.* **83,** 6470–6474
13. Tapley, P., Horwitz, A., Buck, C., Duggan, K., and Rohrschneider, L. (1989) *Oncogene* **4,** 325–333
14. Law, D. A., Nannizzi-Alaimo, L., and Phillips, D. R. (1996) *J. Biol. Chem.* **271,** 10811–10815
15. Miller, L. A., Hong, J. J., Kinch, M. S., Harrison, M. L., and Geahlen, R. L. (1999) *Eur. J. Immunol.* **29,** 1426–1434
16. Ulanova, M., Puttagunta, L., Marcet-Palacios, M., Duszyk, M., Steinhoff, U., Duta, F., Kim, M. K., Indik, Z. K., Schreiber, A. D., and Befus, A. D. (2005) *Am. J. Physiol. Lung Cell Mol. Physiol.* **288,** L497–L507
17. Arias-Salgado, E. G., Lizano, S., Shattil, S. J., and Ginsberg, M. H. (2005) *J. Biol. Chem.* **280,** 29699–29707
18. Arias-Salgado, E. G., Lizano, S., Sarkar, S., Brugge, J. S., Ginsberg, M. H., and Shattil, S. J. (2003) *Proc. Natl. Acad. Sci. U.S.A.* **100,** 13298–13302
19. Klinghoffer, R. A., Sachsenmaier, C., Cooper, J. A., and Soriano, P. (1999) *EMBO J.* **18,** 2459–2471
20. Lowell, C. A. (2004) *Mol. Immunol.* **41,** 631–643
21. Hood, J. D., Frausto, R., Kiosses, W. B., Schwartz, M. A., and Cheresh, D. A. (2003) *J. Cell Biol.* **162,** 933–943
22. Huveneers, S., Arslan, S., van de Water, B., Sonnenberg, A., and Danen, E. H. (2008) *J. Biol. Chem.* **283,** 13243–13251
23. Shattil, S. J. (2005) *Trends Cell Biol.* **15,** 399–403
24. Burridge, K., and Chrzanowska-Wodnicka, M. (1996) *Annu. Rev. Cell Dev. Biol.* **12,** 463–518
25. Clark, E. A., and Brugge, J. S. (1995) *Science* **268,** 233–239
26. Johansson, M. W., Larsson, E., Lüning, B., Pasquale, E. B., and Ruoslahti, E. (1994) *J. Cell Biol.* **126,** 1299–1309
27. Sakai, T., Jove, R., Fässler, R., and Mosher, D. F. (2001) *Proc. Natl. Acad. Sci. U.S.A.* **98,** 3808–3813
28. Sakai, T., Zhang, Q., Fässler, R., and Mosher, D. F. (1998) *J. Cell Biol.* **141,** 527–538
29. Wennerberg, K., Armulik, A., Sakai, T., Karlsson, M., Fässler, R., Schaefer, E. M., Mosher, D. F., and Johansson, S. (2000) *Mol. Cell. Biol.* **20,** 5758–5765
30. Blystone, S. D., Williams, M. P., Slater, S. E., and Brown, E. J. (1997) *J. Biol. Chem.* **272,** 28757–28761
31. Law, D. A., DeGuzman, F. R., Heiser, P., Ministri-Madrid, K., Killeen, N., and Phillips, D. R. (1999) *Nature* **401,** 808–811
32. Chen, H., Zou, Z., Sarratt, K. L., Zhou, D., Zhang, M., Sebzda, E., Hammer, D. A., and Kahn, M. L. (2006) *Genes Dev.* **20,** 927–932
33. Czuchra, A., Meyer, H., Legate, K. R., Brakebusch, C., and Fässler, R. (2006) *J. Cell Biol.* **174,** 889–899
34. Chandhoke, S. K., Williams, M., Schaefer, E., Zorn, L., and Blystone, S. D. (2004) *J. Cell Sci.* **117,** 1431–1441
35. Gao, C., Schaefer, E., Lakkis, M., and Blystone, S. D. (2005) *J. Biol. Chem.* **280,** 15422–15429
36. Butler, B., and Blystone, S. D. (2005) *J. Biol. Chem.* **280,** 14556–14562
37. Prasad, K. S., Andre, P., He, M., Bao, M., Manganello, J., and Phillips, D. R. (2003) *Proc. Natl. Acad. Sci. U.S.A.* **100,** 12367–12371
38. Cowan, K. J., Law, D. A., and Phillips, D. R. (2000) *J. Biol. Chem.* **275,** 36423–36429
39. Kirk, R. I., Sanderson, M. R., and Lerea, K. M. (2000) *J. Biol. Chem.* **275,** 30901–30906
40. Jenkins, A. L., Nannizzi-Alaimo, L., Silver, D., Sellers, J. R., Ginsberg, M. H., Law, D. A., and Phillips, D. R. (1998) *J. Biol. Chem.* **273,** 13878–13885

41. Xi, X., Flevaris, P., Stojanovic, A., Chishti, A., Phillips, D. R., Lam, S. C., and Du, X. (2006) *J. Biol. Chem.* **281,** 29426–29430
42. Datta, A., Huber, F., and Boettiger, D. (2002) *J. Biol. Chem.* **277,** 3943–3949
43. Oxley, C. L., Anthis, N. J., Lowe, E. D., Vakonakis, I., Campbell, I. D., and Wegener, K. L. (2008) *J. Biol. Chem.* **283,** 5420–5426
44. Anthis, N. J., Wegener, K. L., Ye, F., Kim, C., Goult, B. T., Lowe, E. D., Vakonakis, I., Bate, N., Critchley, D. R., Ginsberg, M. H., and Campbell, I. D. (2009) *EMBO J.* **28,** 3623–3632
45. Seeliger, M. A., Young, M., Henderson, M. N., Pellicena, P., King, D. S., Falick, A. M., and Kuriyan, J. (2005) *Protein Sci.* **14,** 3135–3139
46. Wishart, D. S., Bigam, C. G., Yao, J., Abildgaard, F., Dyson, H. J., Oldfield, E., Markley, J. L., and Sykes, B. D. (1995) *J. Biomol. NMR* **6,** 135–140
47. Delaglio, F., Grzesiek, S., Vuister, G. W., Zhu, G., Pfeifer, J., and Bax, A. (1995) *J. Biomol. NMR* **6,** 277–293
48. Vranken, W. F., Boucher, W., Stevens, T. J., Fogh, R. H., Pajon, A., Llinas, M., Ulrich, E. L., Markley, J. L., Ionides, J., and Laue, E. D. (2005) *Proteins* **59,** 687–696
49. Ayed, A., Mulder, F. A., Yi, G. S., Lu, Y., Kay, L. E., and Arrowsmith, C. H. (2001) *Nat. Struct. Biol.* **8,** 756–760
50. Ulmer, T. S., Yaspan, B., Ginsberg, M. H., and Campbell, I. D. (2001) *Biochemistry* **40,** 7498–7508
51. Shaw, S. K., and Brenner, M. B. (1995) *Semin. Immunol.* **7,** 335–342
52. Potter, M. D., Barbero, S., and Cheresh, D. A. (2005) *J. Biol. Chem.* **280,** 31906–31912
53. Hussain, A., Cao, D., and Peng, J. (2007) *Planta* **226,** 475–483
54. Ling, Y., Maile, L. A., Badley-Clarke, J., and Clemmons, D. R. (2005) *J. Biol. Chem.* **280,** 3151–3158
55. García-Alvarez, B., de Pereda, J. M., Calderwood, D. A., Ulmer, T. S., Critchley, D., Campbell, I. D., Ginsberg, M. H., and Liddington, R. C. (2003) *Mol. Cell* **11,** 49–58
56. Hodivala-Dilke, K. M., McHugh, K. P., Tsakiris, D. A., Rayburn, H., Crowley, D., Ullman-Culleré, M., Ross, F. P., Coller, B. S., Teitelbaum, S., and Hynes, R. O. (1999) *J. Clin. Invest.* **103,** 229–238
57. Zou, Z., Chen, H., Schmaier, A. A., Hynes, R. O., and Kahn, M. L. (2007) *Blood* **109,** 3284–3290
58. Clemmons, D. R., and Maile, L. A. (2005) *Mol. Endocrinol.* **19,** 1–11
59. Senis, Y. A., Antrobus, R., Severin, S., Parguiña, A. F., Rosa, I., Zitzmann, N., Watson, S. P., and García, A. (2009) *J. Thromb. Haemost.* **7,** 1718–1726
60. Uhlik, M. T., Temple, B., Bencharit, S., Kimple, A. J., Siderovski, D. P., and Johnson, G. L. (2005) *J. Mol. Biol.* **345,** 1–20
61. Koradi, R., Billeter, M., and Wüthrich, K. (1996) *J. Mol. Graph.* **14,** 51–55

SUPPLEMENTARY DATA

SUPPLEMENTARY FIGURE 1. Mutations for studying phosphorylation. (A) The structures of tyrosine and two amino acids that a tyrosine residue is often substituted with in functional studies: phenylalanine and alanine. Phenylalanine is identical to tyrosine, with the exception of the absence of the phosphorylatable hydroxyl group. Thus, a phenylalanine mutation is often used to make the residue non-phosphorylatable. Alanine, on the other hand, lacks the aromatic ring present in tyrosine and phenylalanine, so a mutation to alanine effectively removes the tyrosine side chain. (B) The structures of glutamate, phosphoserine, phosphothreonine, and phosphotyrosine. A comparison of these structures reveals why glutamate is often used to mimic phosphoserine or phosphothreonine. The negative charge in glutamate is centered about the carboxyl carbon atom, which is located three bonds from Cα. Analogously, the phosphorous atom—around which the negative charge is centered in phosphoserine and phosphothreonine—is also located three bonds away from Cα. In phosphotyrosine, however, this negative center is located seven bonds away from Cα, and these two residues display few other structural similarities, indicating that there is not a sound structural basis for the use of glutamate as a phosphotyrosine-mimicking substitution.

SUPPLEMENTARY FIGURE 2. Unsuccessful and successful attempts at producing tyrosine-phosphorylated β3 integrin tails. (A) Initial attempts at producing tyrosine-phosphorylated integrin tails used full-length c-Src from Upstate (now Millipore) in a method similar to that described in Experimental Procedures, but using much less Src. This panel shows an HPLC chromatograph of β3 Y759F after incubation with c-Src. Molecular weights were determined by mass spectrometry. This chromatograph demonstrates that c-Src will phosphorylate β3 and that the phosphorylated product can be separated from the unphosphorylated tail, but that the reaction is relatively inefficient. The total amount of integrin tail in this experiment would have been approximately enough for one NMR experiment. However, only a small fraction of the integrin was phosphorylated. Producing just this small amount required 1.5 units (2 μg) of Src (costing roughly 50 GBP). Due to the low efficiency of this reaction, producing just one NMR sample by this method would require several fold more material—and would cost several hundred or even thousands of pounds. (B) A second approach attempted was *in vivo* tyrosine phosphorylation in *E. coli*. For this purpose, TKB1 cells (Stratagene) were used, which express trp-inducible Elk, a promiscuous tyrosine kinase (62). This panel shows a representative bacterial growth curve of *E. coli* TKB1 coexpressing GST-tagged β3 Y759F and the tyrosine kinase Elk. Note that bacterial growth is relatively unaffected by the induction of β3 but is significantly curtailed by the induction of Elk. Due to the toxicity of this tyrosine kinase to the bacteria, yields were low and not sufficient for NMR experiments. (C) By producing c-Src kinase domain and using it to phosphorylate integrin tails as described in Experimental Procedures, we were able to produce sufficient quantities of integrin tails for NMR experiments. This panel shows HPLC chromatographs of β3 Y759F after incubation with or without c-Src kinase domain. Note that now roughly half of the β3 has been phosphorylated. Experience indicates that the efficiency of this reaction is limited primarily by integrin solubility (i.e. efficiency approaches 100% when the entire population of the integrin tail remains in solution, which was not the case in this specific example). This experiment produced NMR-scale quantities of phosphorylated integrin tail and only consumed a small fraction of the total c-Src kinase domain purified from 1 L of *E. coli* culture.

SUPPLEMENTARY FIGURE 3. *In vitro* phosphorylation of β integrin tails observed by autoradiography. Autoradiographs of various β integrin tail constructs after phosphorylation in the presence of [γ-32P]ATP with full-length c-Src from Upstate (now Millipore). Samples underwent SDS-PAGE and were then visualized with a PhosphorImager. (A) β1A and β3 integrin tails were incubated with 0.00063, 0.002, or 0.0063 U/μL c-Src. Autophosphorylated c-Src can be observed near the top of the gel. These results indicate that c-Src is capable of phosphorylating both integrins. (B) β3 WT, Y747F, and Y759F were incubated with 0.001 or 0.0025 U/μL c-Src. The lower band is from a photo of the same gel

stained with Coomasie blue in order to observe total protein. These results indicate that c-Src is capable of phosphorylating both the nMD and fMD sites in β3.

SUPPLEMENTARY FIGURE 4. Chemical shift perturbation experiments with integrin tails. (A) ^{1}H-^{15}N HSQC spectra of 0.05 mM ^{15}N-labelled β3 tail with increasing concentrations of Dok1 PTB domain: 0 mM (red), 0.2 mM (yellow), 0.4 mM (green), 0.6 mM (blue), 1 mM (magenta). (B) ^{1}H-^{15}N HSQC spectra of 0.05 mM ^{15}N-labelled β3 tail Y759F pY747 with increasing concentrations of Dok1 PTB domain: 0 mM (red), 0.025 mM (tomato), 0.05 mM (orange), 0.075 mM (yellow), 0.1 mM (green), 0.25 mM (blue), 0.5 mM (purple), 1 mM (magenta). A few peaks broaden out due to intermediate exchange, but these can still be traced when the contour levels are taken lower. (C) Binding curves used for K_d calculation. Peaks were tracked through HSQC spectra of ^{15}N-labelled β3 tail acquired with increasing concentrations of Dok1 PTB domain. For each trackable peak, the change in chemical shift was normalized to the change at 1 mM Dok1, adjusted based on the maximal perturbation observed in that titration. Note that while K_d values were determined by fitting several curves simultaneously, for clarity each value plotted here shows the average of several peaks ± standard error.

SUPPLEMENTARY FIGURE 5. Chemical shift perturbations observed in unphosphorylated integrin tails upon addition of Dok1 PTB domain. Weighted chemical shift maps of perturbations observed in ^{1}H-^{15}N HSQC spectra of unphosphorylated β3, β1A, and β7 tails (50 μM) upon the addition of Dok1 PTB domain (1 mM). Note that the y-axis scale differs between graphs.

SUPPLEMENTARY FIGURE 6. Glutamate does not mimic phosphotyrosine. Weighted chemical shift maps of perturbations observed in ^{1}H-^{15}N HSQC spectra of the β3 tail WT, Y747E, Y747A, and Y759F pY747 (50 μM) upon the addition of (A) 1 mM talin1 F3 domain or (B) 1 mM Dok1 PTB domain. Grey bars correspond to residues that could not be tracked due to exchange broadening. Note that the y-axis scale differs between panels. Also, note that while all three mutations/modifications have a similar effect on the interaction with talin1, the shift map of Dok1 interacting with the Y747E mutant looks most similar to that involving the Y747A mutant and does not resemble in any way the shift map involving the phosphorylated integrin. The full perturbation map for the titration of β3 Y759F pY747 with Dok1 can be seen in Fig. 5.

SUPPLEMENTARY REFERENCES

62. Lhotak, V., Greer, P., Letwin, K., and Pawson, T. (1991) *Mol Cell Biol* **11**, 2496-2502

Supplementary Figure 1

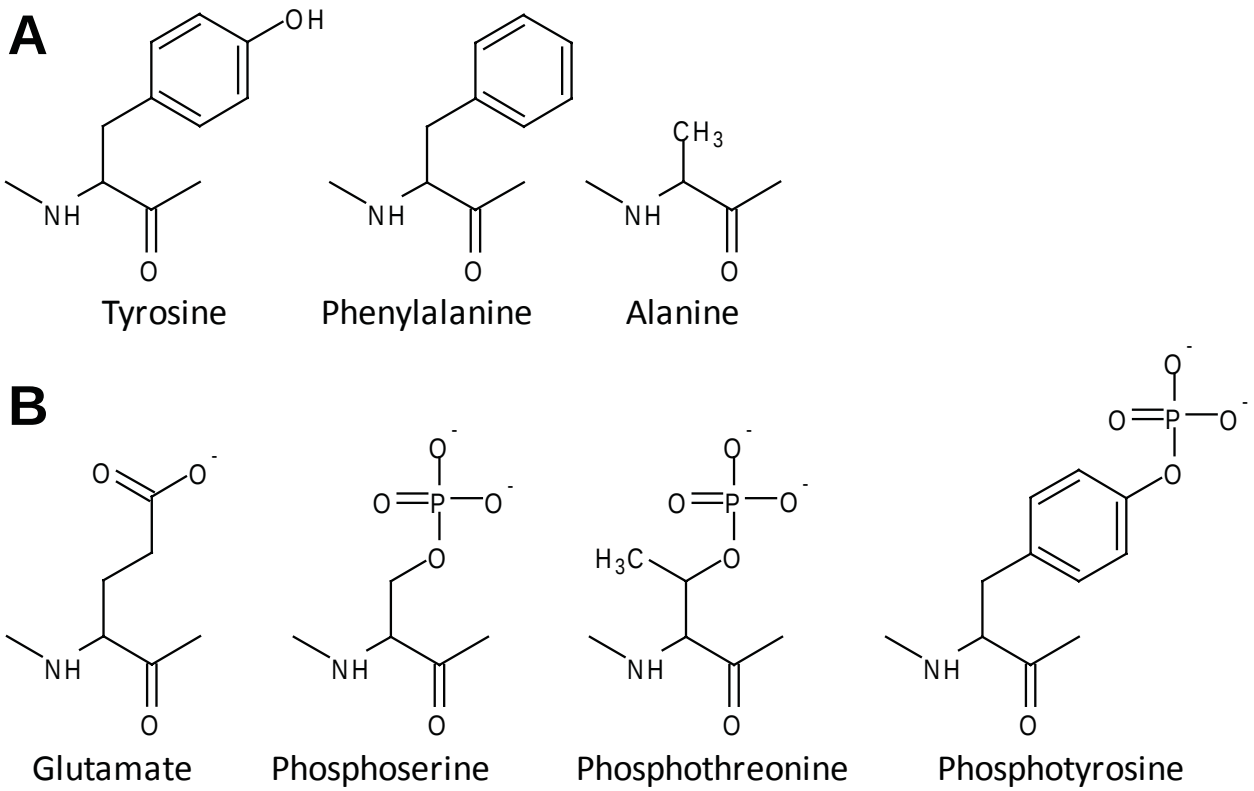

Supplementary Figure 2

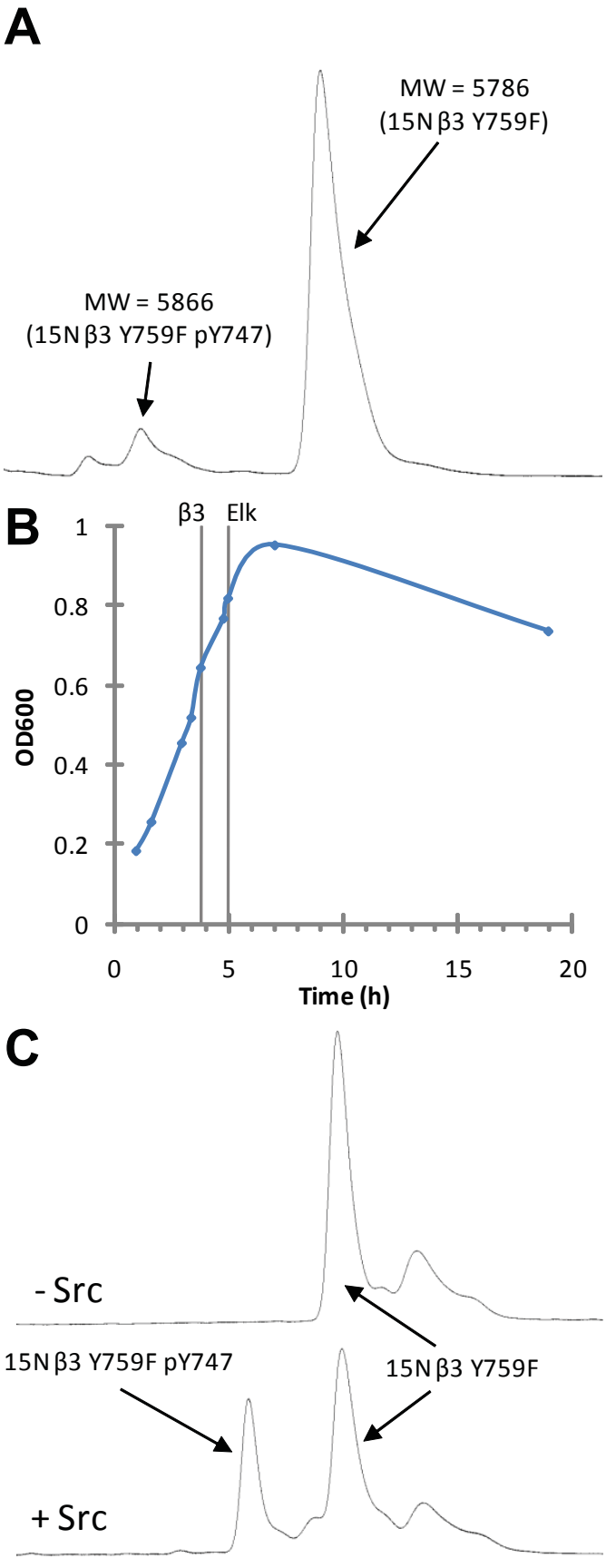

Supplementary Figure 3

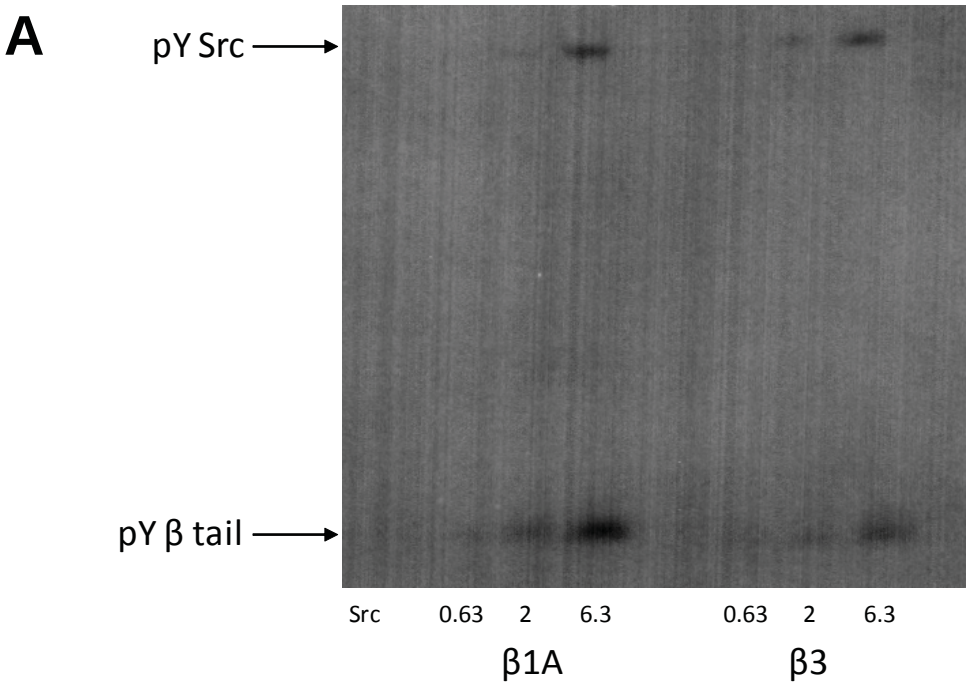

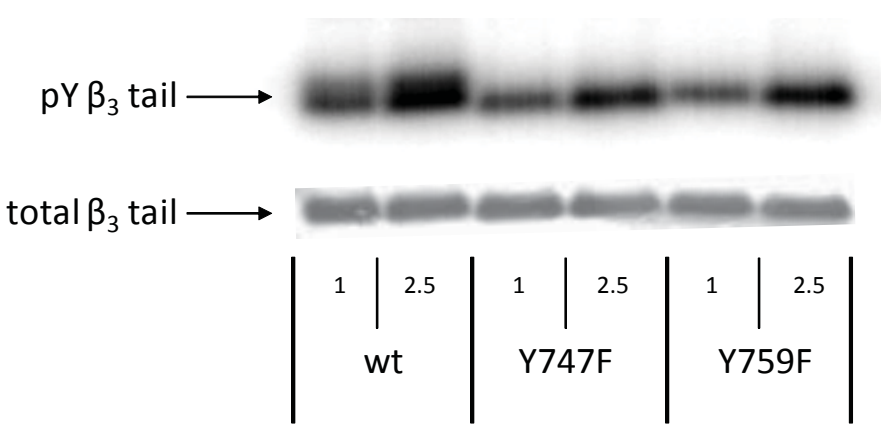

Supplementary Figure 4

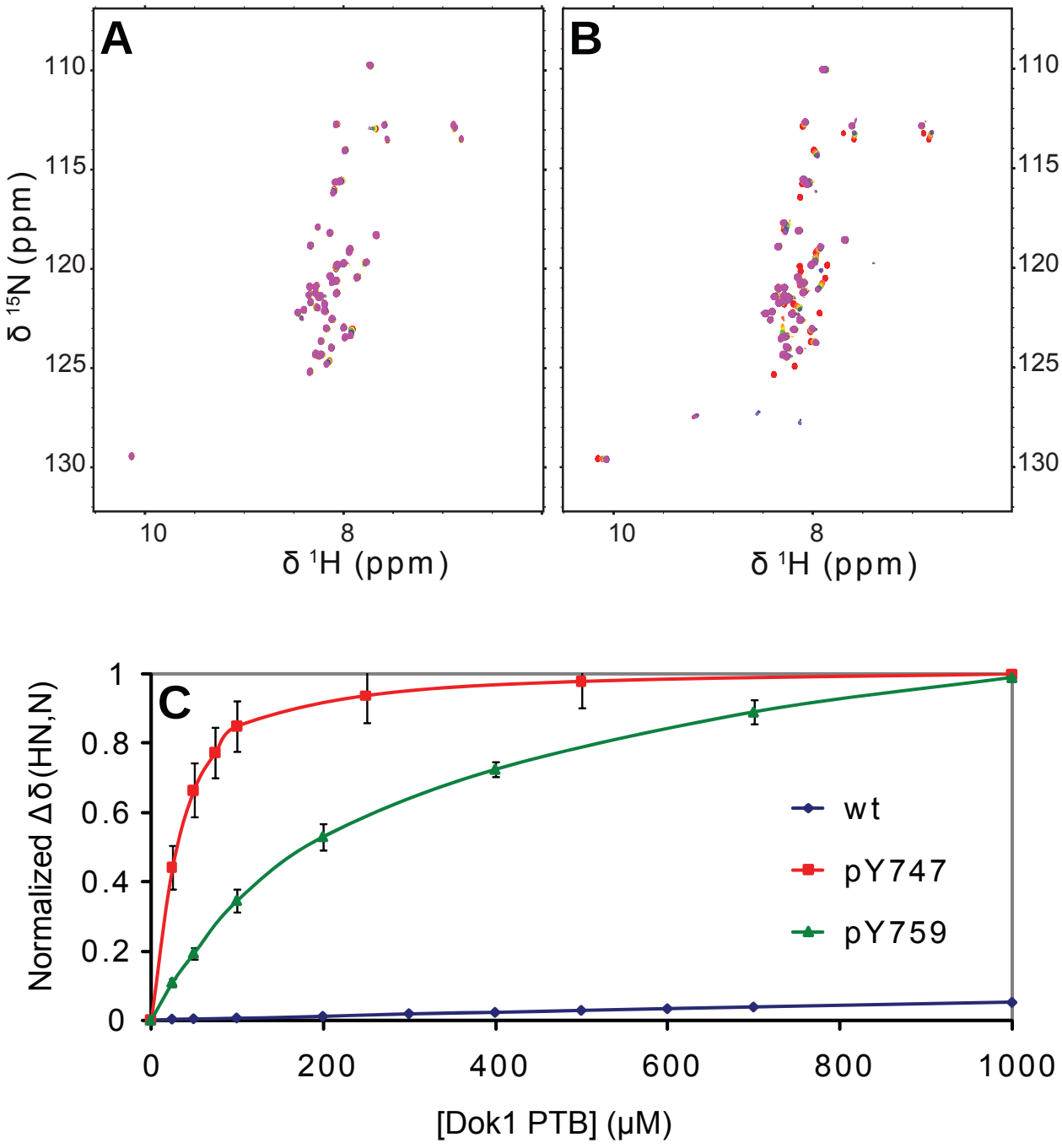

Supplementary Figure 5

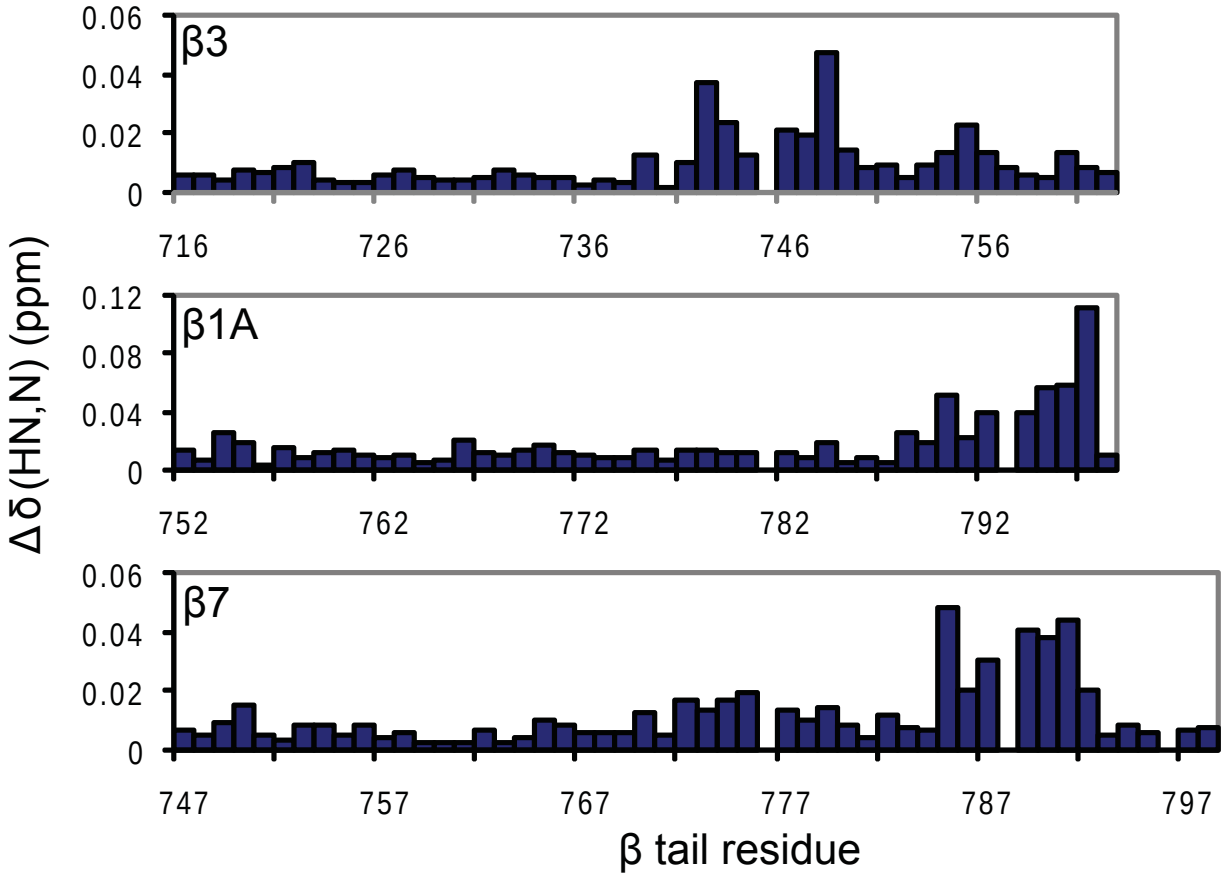

Supplementary Figure 6